

Nanotubes and nanowires

C N R RAO* and A GOVINDARAJ
Solid State and Structural Chemistry Unit, Indian Institute of Science,
Bangalore 560 012, India and CSIR Centre of Excellence in Chemistry,
Jawaharlal Nehru Centre for Advanced Scientific Research, Jakkur,
Bangalore 560 064, India
e-mail: cnrrao@jnrcasr.ac.in

Abstract. Synthesis and characterization of nanotubes and nanowires constitute an important part of nanoscience since these materials are essential building units for several devices. We have prepared aligned carbon nanotube bundles and Y-junction nanotubes by the pyrolysis of appropriate organic precursors. The aligned bundles are useful for field emission display while the Y-junction nanotubes are likely to be useful as nanochips since they exhibit diode properties at the junction. By making use of carbon nanotubes, nanowires of metals, metal oxides and GaN have been obtained. Both the oxide and GaN nanowires are single crystalline. Gold nanowires exhibit plasmon bands varying markedly with the aspect ratio. GaN nanowires show excellent photoluminescence characteristics. It has been possible to synthesise nanotubes and nanowires of metal chalcogenides by employing different strategies.

Keywords. Nanotubes; nanowires; Y-junction; GaN; metal chalcogenides; metal oxides.

1. Introduction

Soon after laboratory preparations of C₆₀ and C₇₀ were reported, carbon nanotubes were discovered as a microscopic wonder¹. Since then, there has been considerable work on carbon nanotubes (CNTs). Multi-walled and single-walled CNTs have been prepared by a variety of methods and several unique properties as well as applications discovered². In this laboratory, we have been working on various aspects of CNTs since the early days. Of particular significance is the discovery of a new route to CNTs by employing organometallic precursors such as metallocenes. This route has not only enabled the preparation of multi-walled and single-walled nanotubes, but also that of aligned nanotube bundles³. What is even more noteworthy is the synthesis of Y-junction nanotubes, which are expected to be crucial components in nanoelectronics⁴. We describe the synthesis and characterization of aligned nanotube bundles and Y-junction nanotubes in this article.

Carbon nanotubes can be usefully employed for the synthesis of other nanomaterials. Thus, metal nanowires can be made inside single-walled CNTs⁵. We have used CNTs as templates to prepare nanotubes and nanowires of several metal oxides⁶ as well as that of GaN⁷, the latter being a very important electronic material

*For correspondence

today. Besides discussing the various types of nanowires prepared by us, we also briefly present a few of the inorganic nanotubes prepared by other methods.

2. Experimental

In order to prepare aligned multi-walled carbon nanotube bundles by ferrocene pyrolysis, the set-up shown in figure 1a was employed. The pyrolysis set-up consists of stainless steel gas flow lines and a two-stage furnace system fitted with a quartz tube (10 mm inner diameter). The flow rate of the gases was controlled using UNIT mass flow controllers. A known quantity (100 mg) of ferrocene (presublimed 99.99% purity) was taken in a quartz boat and placed at the centre of the first furnace. The part of the quartz tube containing the ferrocene was heated by raising the temperature of the first furnace to 673 K at a controlled heating rate. Argon (Ar) gas was passed through the same quartz tube at the desired rate. The ferrocene sublimed and the vapour was carried by the Ar gas into the second furnace, maintained at 1373 K, where pyrolysis occurred. Large quantities of carbon deposits accumulated at the inlet of the second furnace. The main variables in the experiments were the rate of heating of ferrocene, the rate of flow of Ar gas and the

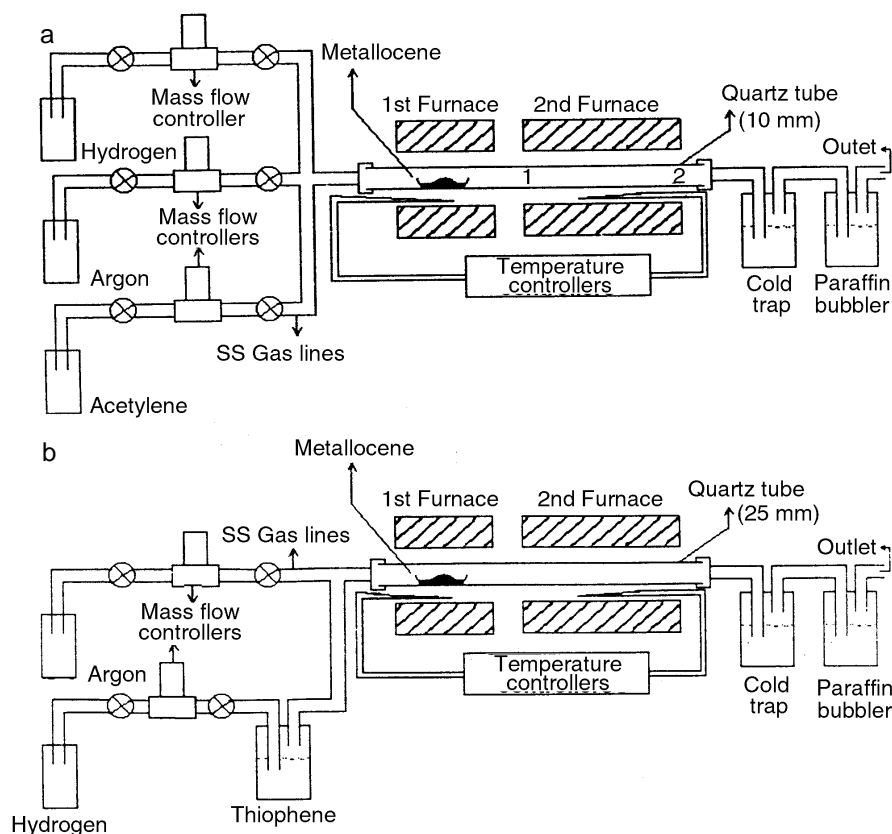


Figure 1. Pyrolysis apparatus employed for the synthesis of (a) aligned carbon nanotube bundles, and (b) Y-junction nanotubes.

pyrolysis temperature. To get aligned nanotube bundles, a typical heating rate of 50 K/min of the first furnace and Ar flow rate of 1000 standard cubic centimetre per minute (sccm) were maintained. To get compact aligned nanotube bundles, C_2H_2 (50–100 sccm) was incorporated during the sublimation of ferrocene. These carbon deposits, mainly containing carbon nanotubes, were examined by a Lieca S44I scanning electron microscope (SEM) and a Jeol 3010 transmission electron microscope (TEM).

The experimental set-up employed by us for the synthesis of Y-junction carbon nanotubes is similar to the one described earlier for the synthesis of aligned nanotube bundles with an additional thiophene bubbler attached to the hydrogen gas line as shown in figure 1b. A known quantity of metallocene was sublimed in the first furnace and carried along with a flow of argon (Ar) gas to the pyrolysis zone in the second furnace. Simultaneously hydrogen (H_2) was bubbled through thiophene and was mixed with the argon–metallocene vapours at the inlet of the furnace and carried to the pyrolysis zone. Pyrolysing these mixed vapors at 1273 K yielded Y-junction nanotubes. Several experiments were carried out by varying the flow rate of Ar and H_2 between 100 and 200 sccm, and 150 and 50 sccm respectively (sccm = standard cubic centimeter per minute). The pyrolysis of Ni/Fe phthalocyanine mixture with thiophene was carried out in a similar manner taking phthalocyanines instead of metallocenes. Carbon deposits accumulating at the inlet and the outlet of the second furnace were examined by TEM and other techniques.

The pyrolysis of thiophene was carried out over Ni/SiO₂ prepared by the following procedure. About 2.4 g of nickel acetate (corresponding to 0.01 mol) was dissolved in 5 ml of acidified ethanol followed by the addition of 2 ml of tetraethyl orthosilicate (TEOS) and stirred for 5 min. To this homogeneous solution, 1.5 ml of HF (38%) was added drop-wise and the resultant mixture was stirred at 323 K till it resulted in the formation of a gel. The gel was dried in an oven at 348 K for 24 h, calcined at 623 K for 2 h and reduced in H_2 atmosphere for 2 h. The temperature was subsequently raised to 1273 K and thiophene vapours were passed over the catalyst for 20 min, by bubbling H_2 (50 sccm) through the thiophene. The sample collected from the boat was observed under the microscope. Similar experiments were also carried out with a Fe/SiO₂ catalyst.

Metal nanowires were produced by two different methods. In the first method we carried out the pyrolysis of metallocenes (e.g. ferrocene) at 1173 K under vacuum (10^{-5} torr) to yield carbon-coated metal (e.g. iron) nanowires. In the second method, we produced nanowires of Au, Ag, Pt and Pd (1.0–1.4 nm dia) in the capillaries of single-walled carbon nanotubes (SWNTs). These SWNTs were produced by the DC arc discharge method using a composite graphite rod containing Y_2O_3 (1 at%) and Ni (4.2 at%) as the anode and a graphite rod as the cathode, under a helium pressure of 660 torr with a current of 100 A and 30 V. The web produced from the arc-discharge predominantly contained SWNT bundles and amorphous carbon, along with metal encapsulated carbon particles. Purification of the web to produce highly pure SWNTs was carried out as follows. The as-produced web containing SWNTs was heat-treated at 573 K in air for 24 h to remove the amorphous carbonaceous materials. The heat-treated material was stirred with concentrated nitric acid at 333 K for about 12 h and washed with distilled water to remove the dissolved metal particles. The SWNT material so obtained was suspended in ethanol by using an ultrasonicator and filtered through a micropore filter paper (0.3 μ m) from Millipore

to remove the polyhedral carbon particles present. The product was then dried at 423 K for about 12 h. Purified SWNT samples so obtained were heat-treated at 623 K for 30 min to remove the acid sites on the surface of the tubes. This treatment is known to open the nanotubes. High resolution electron microscopic (HREM) observations were carried out to confirm these are indeed purified SWNT samples.

In order to prepare gold nanowires, 5 mg of purified SWNTs was mixed with ~10 mg of $\text{HAuCl}_4 \cdot x\text{H}_2\text{O}$ and the mixture dried in a 10 mm diameter quartz tube at 373 K for 2 h under vacuum (10^{-3} torr). The quartz tube was sealed under vacuum and heated at 643 K (decomposition temperature of AuCl_3 is 527 K) for 20 h. In order to prepare Pt nanowires, a mixture of SWNTs (5 mg) with $\text{H}_2\text{PtCl}_6 \cdot 6\text{H}_2\text{O}$ (10 mg) was dried at 393 K for 2 h under vacuum and the sealed quartz containing the mixture heated in a furnace at 773 K (melting point of $\text{H}_2\text{PtCl}_6 \cdot 6\text{H}_2\text{O}$ is 333 K) for 20 h. In a similar manner, PdCl_2 (10 mg) was mixed with the SWNTs (5 mg) and heated at 373 K for 2 h and sealed under vacuum. The sealed tube was maintained at 873 K (decomposition temperature of PdCl_2 is 773 K) for 20 h. In all the sealed tube reactions, temperature was maintained at ~100 K above the decomposition (or melting point) of the respective metal salt. After treatment with metal salts, the sealed tubes were broken open and the product treated with hydrogen at 723 K for one hour to reduce the metal salt present. The hydrogen treatment was not found to be essential in the case of gold nanowires. In order to prepare Pt nanowires we have employed a simple solution method as well. The mixture of SWNTs (5 mg), $\text{H}_2\text{PtCl}_6 \cdot 6\text{H}_2\text{O}$ (10 mg) was refluxed in concentrated HCl or HNO_3 (2 ml) for 1 h. We have also attempted to prepare metal nanowires by sonochemical means, wherein SWNTs in AgNO_3 solution were sonicated (35 MHz ultrasound treatment) for a few hours in a hydrogen atmosphere. It should be noted that the SWNTs generally get filled by the metal salt/metal through the open ends.

The products obtained from the various processes discussed above were dispersed in carbon tetrachloride and deposited onto holey carbon copper grids for transmission electron microscope (TEM) observations. Plasmon absorption bands of the dispersions of the nanowires in alcohol were recorded using a Hitachi U3400 spectrometer.

The method of preparation of metal oxide nanowires and nanotubes makes use of multi-walled carbon nanotubes (MWNTs). MWNTs were prepared by the arc vaporization of graphite rods in a helium atmosphere (550 torr) at 30 V, 100 A direct current. The nanotubes formed in the core region of the cathode deposit were dispersed in methanol and sonicated for 2 h in a separating funnel. The bulky graphitic carbon was removed from the suspension. The remaining solid suspension was allowed to settle, dried and heated in air at 923 K for 20 min to oxidize the graphitic carbon. The pure carbon nanotubes thus obtained were closed at either end or open at one end at some other instances. They were treated with boiling HNO_3 for 24 h. Such nanotubes are almost always open and contain a considerable number of acidic sites on the surface. The concentration of the surface acidic sites is around 6×10^{20} sites g^{-1} of nanotubes. The acid-treated nanotubes were washed with water and dried in an oven at 333 K for 12 h. The nanotubes so obtained had an inner diameter in the range of 2–8 nm and an outer diameter in the range of 10–30 nm (length up to one μm). The acid-treated carbon nanotubes were coated with an appropriate oxide precursor such as an alkoxide and dried at 373 K, followed by calcination at 723 K. The calcined sample was heated at 973 K in air to burn off the

carbon. While generally we obtained nanowires by this method, in some instances we found nanotubes as well.

The experimental procedure for preparing oxide nanostructures is as follows. In order to prepare V_2O_5 coated carbon nanotubes, aqueous sodium meta-venadate was first passed through a cation exchange column (DOWEX) to get vanadic acid (HVO_3). Acid-treated carbon nanotubes (100 mg) were stirred with 2 ml of HVO_3 for 48 h. The excess gel was removed by washing with water and acetone. The nanotubes so obtained were dried in an oven at 373 K for 6 h.

In the case of WO_3 and MoO_3 , an aqueous solution of Na_2WO_4 or Na_2MoO_4 was passed through a cation exchange column. The resulting tungstic or molybdic acid (H_2WO_4 or H_2MoO_4) was used for coating the acid-treated carbon nanotubes (100 mg) by magnetic stirring for 48 h. The excess tungstic or molybdic acid was washed off with water. The nanotube sample was dried at 373 K for 6 h. To coat the nanotubes with Sb_2O_5 , the acid-treated nanotubes (100 mg) were mixed with 2 ml of $SbCl_5$ and stirred for 48 h. The sample was filtered and washed with methanol and dried at 373 K for 6 h.

In the case of RuO_2 , the gel was obtained by the reaction of aqueous $RuCl_3$ (aldrich) with NaOH. The gel was washed repeatedly with distilled water to remove free Na^+ and Cl^- ions. Acid-treated carbon nanotubes (100 mg) were stirred with the gel for 48 h. The sample was dried at 373 K for 6 h and treated with H_2O_2 to oxidize Ru^{3+} to Ru^{4+} . The resulting nanotubes were dried at 373 K for 6 h and calcined at 723 K for 12 h.

Anhydrous $IrCl_3$ (Aldrich) was fused with NaOH to obtain Na_2IrCl_6 . This was diluted with distilled water to get an intensely blue-coloured solution. Acid-treated carbon nanotubes (100 mg) were stirred with this solution for 48 h. The sample was washed with distilled water and dried at 373 K for 6 h.

After the oxide-coated nanotubes were heated in air at 973 K (except in the case of V_2O_5 where it was 773 K), the oxide nanostructures obtained were subjected to X-ray diffraction (XRD), SEM and TEM.

The procedures employed by us for the preparation of GaN nanowires are as follows. In procedure (i), GaN nanowires were prepared by using multi-walled carbon nanotubes (MWNTs) as templates. In a quartz tube (12 cm length, 6 mm dia.), closed at one end, 100 mg of $Ga(acac)_3$ (gallium acetylacetonate) was taken, above which 25 mg of MWNTs was placed. This tube was placed in a larger diameter quartz tube and was connected to a dynamic NH_3 atmosphere (flow rate: 150 ml min^{-1}) with a suitable T joint arrangement. This quartz tube set-up was then held vertically in a small tubular furnace and was heated to 1183 K and held at that temperature for 3 h. We used MWNTs prepared by arc discharge as well as by hydrocarbon pyrolysis. Aligned MWNTs prepared by pyrolysis of organometallic precursors were also used as templates. The use of activated carbon in place of MWNTs also yielded GaN nanowires.

Procedure (ii) involves two steps. In the first step, a homogeneous mixture of $Fe(acac)_3$ and $Ga(acac)_3$ is prepared in silica gel, followed by calcination and reduction to yield a dispersion of Fe and gallium oxide particles in the gel. The second step involves the reaction with ammonia. The dispersion of gallium oxide and Fe catalyst in silica gel was prepared as follows. $Ga(acac)_3$ (0.991 g) and $Fe(acac)_3$ (0.353 g) (corresponding to 0.3 at% of Ga and 0.1 at% of Fe) were dissolved in 25 ml of methanol. To this solution, 2 ml of tetraethylorthosilicate

(TEOS) was added slowly under stirring. To the resulting solution, 1.5 ml of 30% HF was added drop-wise and stirred for another 30 min to achieve slow gelation. The gel was transferred to a petri dish and dried in an oven at 343 K for 12 h. The dried gel was fragmented into small sections (5–15 mm² area) and calcined under argon at 673 K for 2 h and then reduced in hydrogen at the same temperature for further 2 h, resulting in the formation of a dispersion of Fe particles along with gallium oxide over silica. This material was heated in NH₃ (flow rate: 150 ml min⁻¹) at 1183 K for 4 h. In procedure (iii), a mixture of Ga and Fe oxides was obtained by the decomposition of the mixture of acetylacetonates. This oxide mixture was then reduced in H₂ at 673 K and reacted with NH₃.

Procedure (iv) employs the citrate gel method which allows the formation of fine, high surface area Fe₂O₃/Ga₂O₃ particles. Here 0.281 g of Ga₂O₃ was dissolved in 5 ml of aqua regia and the solution diluted with 15 ml of water. To this solution, 0.404 g of ferric nitrate and equivalent moles of citric acid (4 mmoles) were added. To the homogeneous solution obtained, a solution of ethylene diamine was added drop-wise till the pH rose to 7. The solution was first heated at 333 K for 8 h to obtain a viscous solution and further heated at 353 K for 36 h in an oven to obtain a uniform gel. The gel was dried at 403 K for 24 h and then heated at 453 K for 12 h to yield froth-like material (formed on the beaker). This was calcined at 823 K for 12 h and reduced in H₂ at 673 K for 4 h to yield a fine dispersion of the Fe particles and gallium oxide. This mixture was reacted with NH₃ (flow rate: 150 ml min⁻¹, 1183 K, 4 h).

The synthesis of GaN nanowires was also carried out by using Ni particles in place of Fe particles in procedures (ii), (iii) and (iv), by using Ni(acac)₂ in place of Fe(acac)₃. Some experiments were also conducted with a mixture of H₂ and NH₃ for nitridation, but it was found that H₂ did not affect the nitridation in any way. Similarly, the reduction step with H₂ was not found to be essential. Direct reaction of NH₃ with the metal oxides in procedures (ii)–(iv) also gave GaN nanowires.

X-ray diffraction (XRD) patterns were recorded using the Seifert (XRD, XDL, TT, and Cu target) instrument. Conventional *q-q* scans were collected with the Bragg–Brenatano goniometer and a high resolution, 169 eV Si (Li) solid state detector with 1 mm/2 mm slit. X-ray photoelectron spectra of the GaN nanowire samples recorded with an Escalab MKIV spectrometer employing AlK α radiation (1486.6 eV) gave characteristic signals of Ga and N. Scanning electron microscope (SEM) images were obtained with the Leica S-440I microscope. Transmission electron microscopic (TEM) images were obtained with the Jeol (JEM 3010) operating with an accelerating voltage of 300 kV. Photoluminescence measurements were carried out with a Perkin–Elmer Model LS50B luminescence spectrometer. Scanning tunneling microscope (STM) measurements were carried out with an Omicron instrument.

3. Results and discussion

3.1 Aligned carbon nanotube bundles

In figure 2a we show the SEM image of the nanotubes obtained by carrying out the pyrolysis of ferrocene at 1373 K with a fast heating rate of ferrocene (100 K min⁻¹)

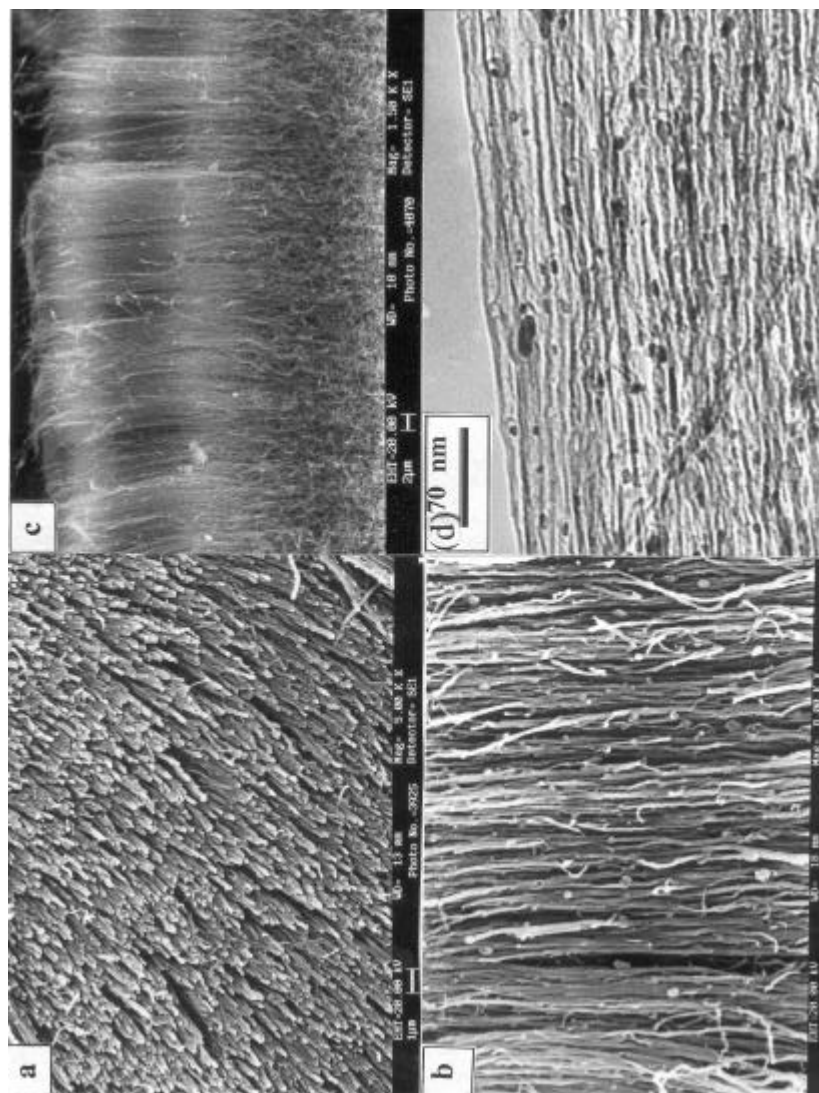


Figure 2. SEM images of aligned nanotubes obtained by the pyrolysis of ferrocene at 1373 K and 1000 sccm Ar: (**a**) and (**b**) show views of the aligned nanotubes along and perpendicular to the axis of the reaction mixture; (**c**) shows the SEM image of aligned nanotubes obtained under a flow of C_2H_2 (5 sccm) and Ar (1000 sccm); and (**d**) shows the SEM image of densely packed aligned nanotubes obtained in the presence of a higher proportion of C_2H_2 (85 sccm) in the reaction mixture.

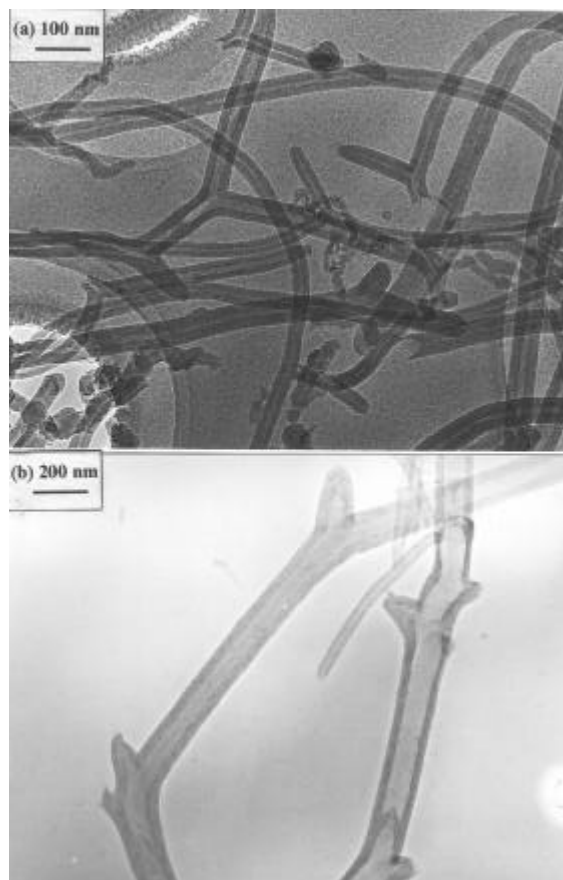


Figure 3. TEM image of Y-junction nanotubes obtained by the pyrolysis of cobaltocene–thiophene mixtures under flow of H_2 (100 sccm) and Ar (150 sccm) (a), and by the pyrolysis of thiophene over the Ni/SiO₂ catalyst under flow of H_2 (50 sccm) and Ar (200 sccm) (b).

and a high flow rate of Ar (1000 sccm). The images in figure 2a and b, which are recorded in two directions with respect to the axis of the nanotubes, clearly reveal the extraordinary alignment. TEM images of these nanotubes reveal that they are multi-walled, some of them partially filled with metallic iron. Pyrolysis of ferrocene at 1170 K under vacuum (10^{-5} torr) also yielded good quantities of aligned nanotube bundles. When the rate of heating of ferrocene (1 K min^{-1}) and the flow rate of Ar (10 sccm) were low, fewer aligned nanotubes were obtained at a pyrolysis temperature of 1373 K. We carried out the pyrolysis of ferrocene with acetylene, by passing a mixture of argon and acetylene through the quartz tube. In figure 2c we show an SEM image of the aligned nanotubes obtained by the pyrolysis of mixture of ferrocene and acetylene (5 sccm) at 1373 K in flowing Ar (1000 sccm). The alignment could be further improved by increasing the flow rate of C_2H_2 . The SEM image in figure 2c shows the densely packed aligned nanotubes. The TEM image in figure 2d reveals how well aligned these nanotubes are. The nanotubes in the bundles were generally closed and were 5–10 μm in length.

3.2 Y-junction carbon nanotubes

Carbon deposits obtained from the pyrolysis of cobaltocene-thiophene mixtures showed Y-junction nanotubes both at the inlet and outlet ends of the second furnace. In figure 3a, we show the Y-junction nanotubes obtained when the flow rates of H₂ and Ar were 100 sccm and 150 sccm respectively. The diameter of the inner core of the nanotubes is 20 nm and the outer diameter is 50 nm. Multiple junctions are found in the nanotubes at these flow rates. The formation of multiple junctions suggests the possibility of multiple tunnel devices in a single carbon nanotube. When the H₂ flow rate was increased to more than 200 sccm, there was no significant change in the features of the nanotubes. At low flow rates of H₂ (less than 25 sccm), no junction nanotubes were found. When Ar was bubbled through thiophene instead of H₂, there was a greater proportion of amorphous carbon and the junctions obtained were not of good quality. The interlayer separation of the graphitic layer as revealed by HREM as well as electron diffraction (ED) pattern is ~3.4 Å as expected. The graphitic layers are seen parallel to the corners of the junctions although fishbone-type stacking is also present. The presence of graphite layers parallel to the junction is however noteworthy. More detailed studies employing HREM as well as chemical analysis are required to understand the structure and chemical constitution of the junctions. Pyrolysis of ferrocene-thiophene mixtures showed the presence of Y-junctions predominantly in the deposits collected at the outlet ends when the H₂ flow rate used was 25 sccm, that of Ar being 225 sccm. The presence of junctions in the inlet region was rare. The flow rate of H₂ was crucial in the formation of junctions. The use of Fe- and Ni-phthalocyanines instead of metallocenes also yields Y-junctions, with a Ni-phthalocyanine-thiophene mixture at a H₂ flow rate of 50 sccm and that of Ar 200 sccm. When the flow rate of H₂ and Ar were 150 and 100 sccm respectively, multiple junctions formed continuously.

Y-junctions are also obtained by the pyrolysis of thiophene over the Ni/SiO₂ catalyst and the nanotube junctions obtained by this method are as good as those obtained by the pyrolysis of metallocene-thiophene mixtures. The amorphous carbon material was negligible in this procedure. Multiple junction features occur commonly. Long and straight junctions, which are several nanometres in length, are also observed. The walls of the junctions are however significantly thicker than those observed previously. The outer and core diameters of the nanotubes were as high as 136 nm and 55 nm respectively. We obtained good Y-junctions with Fe/SiO₂ catalyst as well. In figure 3b we show a TEM image of the multiple junctions obtained by using the Ni/SiO₂ catalyst. These Y-junctions have an inner diameter of 75 nm and outer diameter of 160 nm. Pyrolysis of CS₂ with nickelocene (flow rate: H₂ = 50 sccm, Ar = 200 sccm) gave good yields of junction nanotubes. Pyrolysis of thiophene with iron pentacarbonyl (Fe(CO)₅) carried out by bubbling H₂ (50–100 sccm) through the Fe(CO)₅ along with Ar (150–200 sccm) bubbled through the thiophene showed the presence of interesting junction structures. We have also carried out the pyrolysis of vapours of acetone and copper (II) acetylacetonate (Cu(acac)₂) to produce Y-junctions. To achieve this, Cu(acac)₂ vapours carried by Ar (flow rate = 200 sccm) was mixed with acetone carried by H₂ (flow rate = 50 sccm) and the mixture pyrolysed at 1273 K. Although this method yielded Y-junctions, they were not as good as those obtained by using metallocenes or the

Fe (Ni)/SiO₂ catalyst. Furthermore, large quantities of amorphous carbon were present in the product.

Tunneling conductance measurements were carried out by positioning a STM tip atop a Y-junction (the point of contact between the three arms) as well as on the individual arms of the Y-junction nanotubes. The I-V curves obtained along the arms of the Y-junction were compared with the I-V curves obtained from atop the Y-junctions. Both the curves were typical of metal-insulator-metal junctions with the current values displaying a threshold around zero bias. The curve along the arm is symmetric about the zero bias. The tunnel current has the same magnitude (~19 nA) at bias voltages of +1700 and -1700 mV. The plot of differential conductance versus bias gives a gap of ~760 mV, symmetric with respect to zero bias. At the junction, however, the threshold bias voltage is ~190 mV in the positive bias and the tunnelling current rises exponentially beyond this bias voltage, reaching a maximum of ~28 nA at 1700 mV. Under a negative bias, there is a gradual rise in the tunnelling current beyond a relatively large threshold bias (~440 mV). The tunneling current reaches a value of ~18 nA at a negative bias of 1700 mV, which is far less than that for the positive bias. Thus, the *I-V* plot at the junction is asymmetric with respect to bias polarity. The plot of differential conductance (*dI/dV*) versus bias also demonstrates the asymmetry about zero bias. Such asymmetry is characteristic of a junction diode and this in turn indicates the existence of intramolecular junction in the carbon nanotubes.

3.3 Metal nanowires

In figure 4a, we show a TEM image which reveals the presence of a large number of gold nanowires obtained from the sealed tube reaction. The image clearly shows extensive filling of SWNT tubes. The length of the gold nanowires is in the range of 15–70 nm and the diameters in the range 1.0–1.4 nm. Detailed TEM observations show that the extent of filling of Au nanowires inside the SWNTs is in excess of 50%. Selected area electron diffraction (SAED) patterns taken from the region of nanowires (see inset of figure 4b) shows diffuse rings due to small polycrystalline metal particles. The diffraction rings corresponds to the (111) and (002) reflections of gold. In some nanowires, however we have found the metal to be single crystalline as shown in the HREM image of figure 4b. This image reveals the resolved lattice of gold with a spacing of ~0.23 nm, corresponding to the (111) planes. Polycrystalline Au aggregates could be transformed into the single crystalline form by suitable annealing. Platinum nanowires obtained by the sealed tube reaction are ~90 nm long and ~1 nm in diameter. Long nanowires of Pt (~70 nm long and ~1 nm dia) were obtained by the solution method as well. Palladium nanowires could also be obtained by the sealed tube reaction, but these were not as long as those of gold or platinum. We could obtain silver nanowires by heating the SWNTs obtained after sonication in AgNO₃ solution at 623 K for 1 h, in a Ar-H₂ atmosphere.

We have recorded the electronic absorption spectra of dispersions of gold nanowires in ethanol. The spectra show transverse and longitudinal plasmon absorption bands. While the transverse absorption band (~520 nm) does not vary with the aspect ratio of Au nanowires, the position of the longitudinal absorption band varies markedly with the aspect ratio and medium dielectric constant.

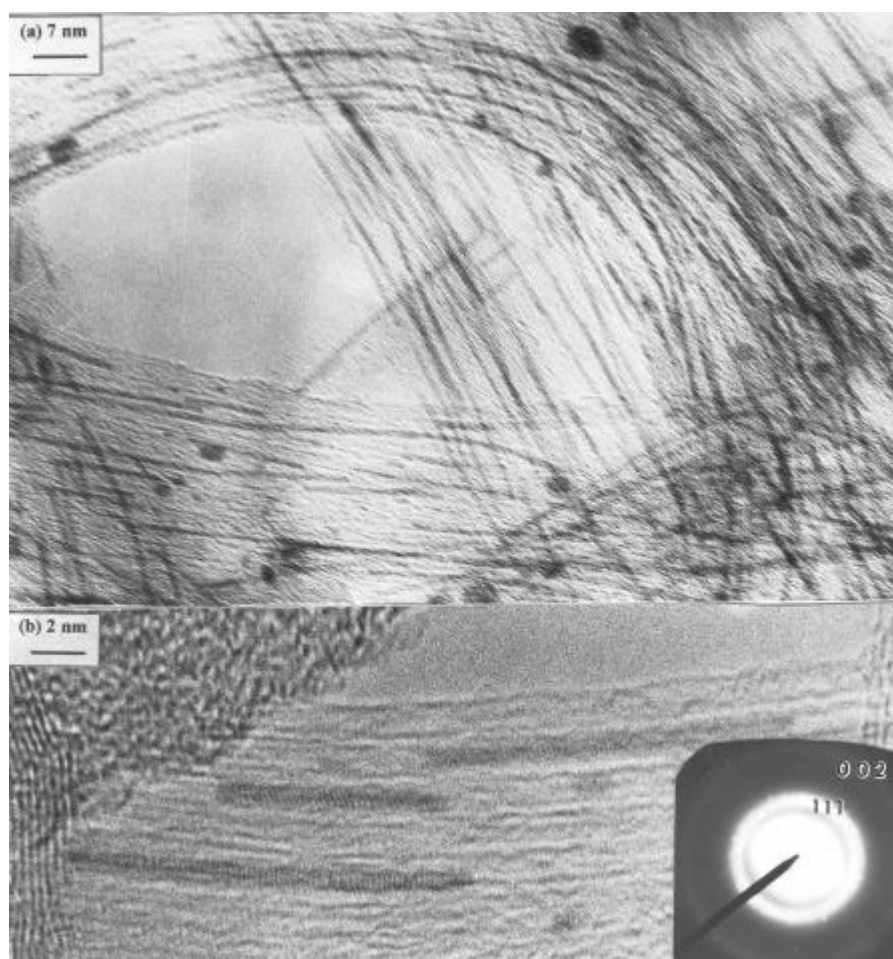


Figure 4. (a) TEM image of Au nanowires inside SWNTs obtained by the sealed-tube reaction, and (b) HREM image showing the single crystalline nature of some of the Au nanowires. Inset in (b) shows an SAED pattern of the nanowires.

Decomposition of the observed band envelopes indicates that the dispersions of Au nanowires are characterized by the bands around 670, 860 and 1150 nm due to the longitudinal absorption. These bands indicate that there is a distribution of aspect ratios in the nanowire dispersion, with the aspect ratio corresponding to the longest wavelength being rather large. We estimate the range of aspect ratios in the nanowire dispersions examined by us to be 3–6. Clearly, more detailed studies of the plasmon bands of metal nanowires would be of value.

3.4 Metal oxide nanowires

Calcined samples of different oxide-coated carbon nanotubes revealed the presence of satisfactory coverage of the oxidic material as shown in the typical TEM images

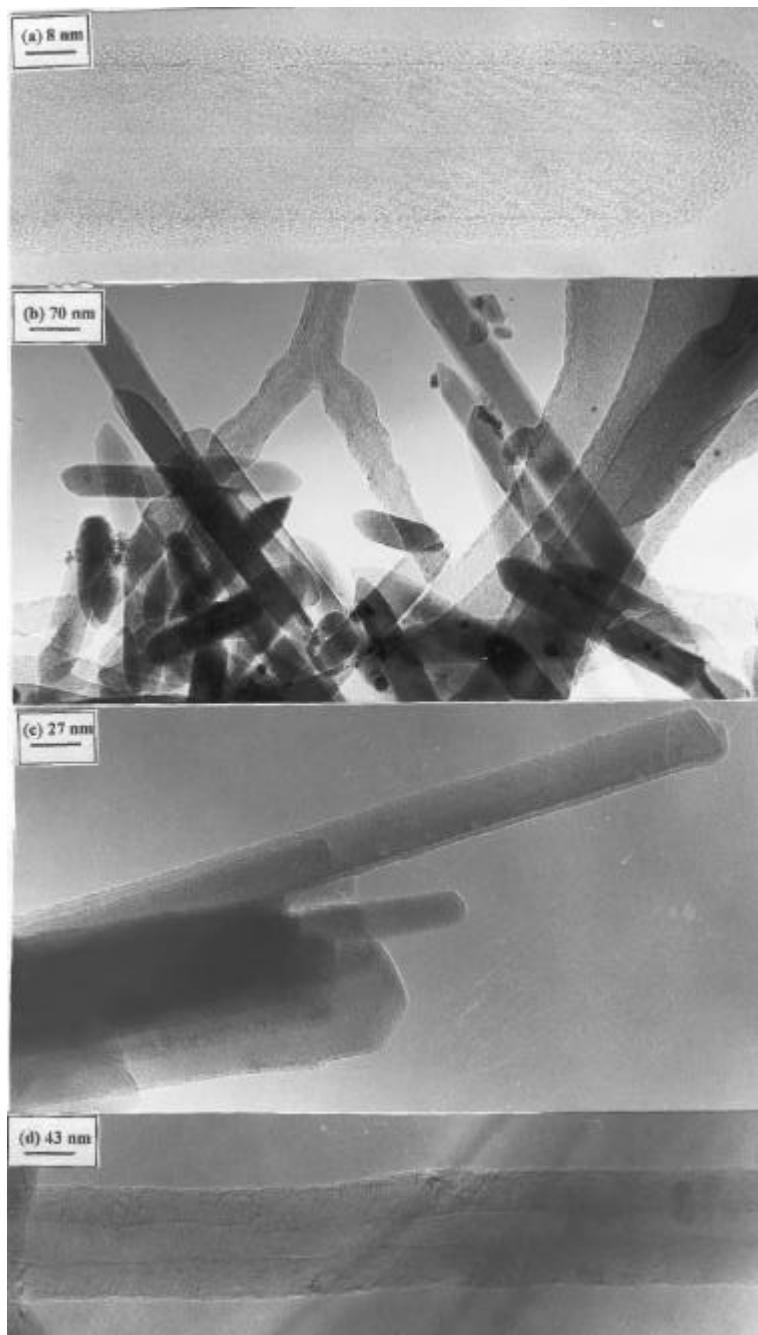


Figure 5. (a) HREM image of a carbon nanotube coated with V_2O_5 , (b) TEM image of V_2O_5 nanowires, (c) TEM image of WO_3 nanowires and (d) TEM image of an MoO_3 nanotube.

in figure 5a. Thus, the high resolution electron microscopic image of the nanotubes coated with V_2O_5 in figure 5a shows that the oxidic coating is uniform throughout the length of the nanotube. The situation is similar with other oxide coatings also. The strong interaction of the oxidic material with the surface of the carbon nanotubes is due to the presence of surface acidic sites, resulting from the acid treatment. On the removal of the nanotube template, the resulting oxidic species showed the presence of interesting nanostructures. In figure 5b we show the TEM bright field image of the V_2O_5 nanowires obtained after the removal of the template. The image shows the presence of copious quantities of nanowires. The nanowires have diameters in the range of 20–25 nm and are 2–3 μm long. The selected area electron diffraction pattern (SAED) on a nanowires shows the presence of regular spots due to (110) and (200) planes signifying the single crystal nature of the V_2O_5 nanowires. The zone axis projection is along [102] of the orthorhombic V_2O_5 . The XRD pattern of the oxide powder showed it to be orthorhombic, with unit cell parameters of $a = 11.44 \text{ \AA}$, $b = 3.54 \text{ \AA}$ and $c = 4.35 \text{ \AA}$, in agreement with the literature values (JCPDS file: 9-387). The template could be removed at a relatively lower temperature in the case of V_2O_5 , since it catalyzes the oxidation of the nanotubes. In the case of WO_3 , SEM observations indicated a relatively good yield of the nanowires. A typical high resolution TEM image of the WO_3 nanowires showed a relatively long nanowire, with a length of 5 μm . In figure 5c we show a bunch of nanowires having diameters in the range of 30–80 nm. The SAED pattern indicates a zone axis projection along [010], with the Bragg spots corresponding to the (001) and (200) planes of monoclinic WO_3 . The XRD pattern of the oxide powder gave unit cell parameters of the monoclinic phase ($a = 7.331 \text{ \AA}$, $b = 7.52 \text{ \AA}$ and $c = 7.71 \text{ \AA}$ with $\beta = 90.1^\circ$, JCPDS file: 24-747).

We obtained nanowires of MoO_3 in high yields (after template removal at 873 K for 12 h). In addition in some of the preparations we have also obtained nanotube structures as revealed by the TEM image in figure 5d. SEM image of the MoO_3 nanowires is shown in figure 6a. The diameter of the nanowires is in the 80–150 nm range, with length in the 5–15 μm range. By subjecting the MoO_3 -coated carbon nanotubes to repeated washing (before calcination), we are able to obtain thinner nanowires of the oxide, after removal of the template. The SAED pattern reveals the single crystalline nature of the nanowire. The XRD pattern gave the orthorhombic unit cell parameters, $a = 3.96 \text{ \AA}$, $b = 13.85 \text{ \AA}$ and $c = 3.7 \text{ \AA}$ (JCPDS file: 35-609). Sb_2O_5 gave nanowires in relatively good yields. The nanowires have diameters in the range of 10–60 nm and lengths in the range 100–400 nm. The SAED pattern also shows bright spots due to (222) planes. The XRD pattern showed it to have a cubic structure with the cell parameter, $a = 10.98 \text{ \AA}$ (JCPDS file: 5-534).

While the oxide nanostructures discussed above are all nonmetallic, we sought to prepare nanowires of metallic oxides such as MoO_2 , RuO_2 and IrO_2 . In order to obtain MoO_2 nanowires, nanowires of MoO_3 were reacted with hydrogen at 773 K for 48 h. The SEM and TEM images of MoO_2 nanowires showed that these have diameters in the 150–300 nm range and length in the 5–15 μm range. The XRD patterns showed the presence of a monoclinic phase with the unit cell parameters, $a = 5.60 \text{ \AA}$, $b = 4.85 \text{ \AA}$, $c = 5.54 \text{ \AA}$ with $\beta = 119.4^\circ$ (JCPDS file: 32-671). HRTEM images and SAED pattern of the RuO_2 nanowires showed these are indeed single-crystalline, the lattice planes with $d = 3.1 \text{ \AA}$ corresponding to (110) planes of tetragonal RuO_2 . The XRD patterns confirmed tetragonal structure with the

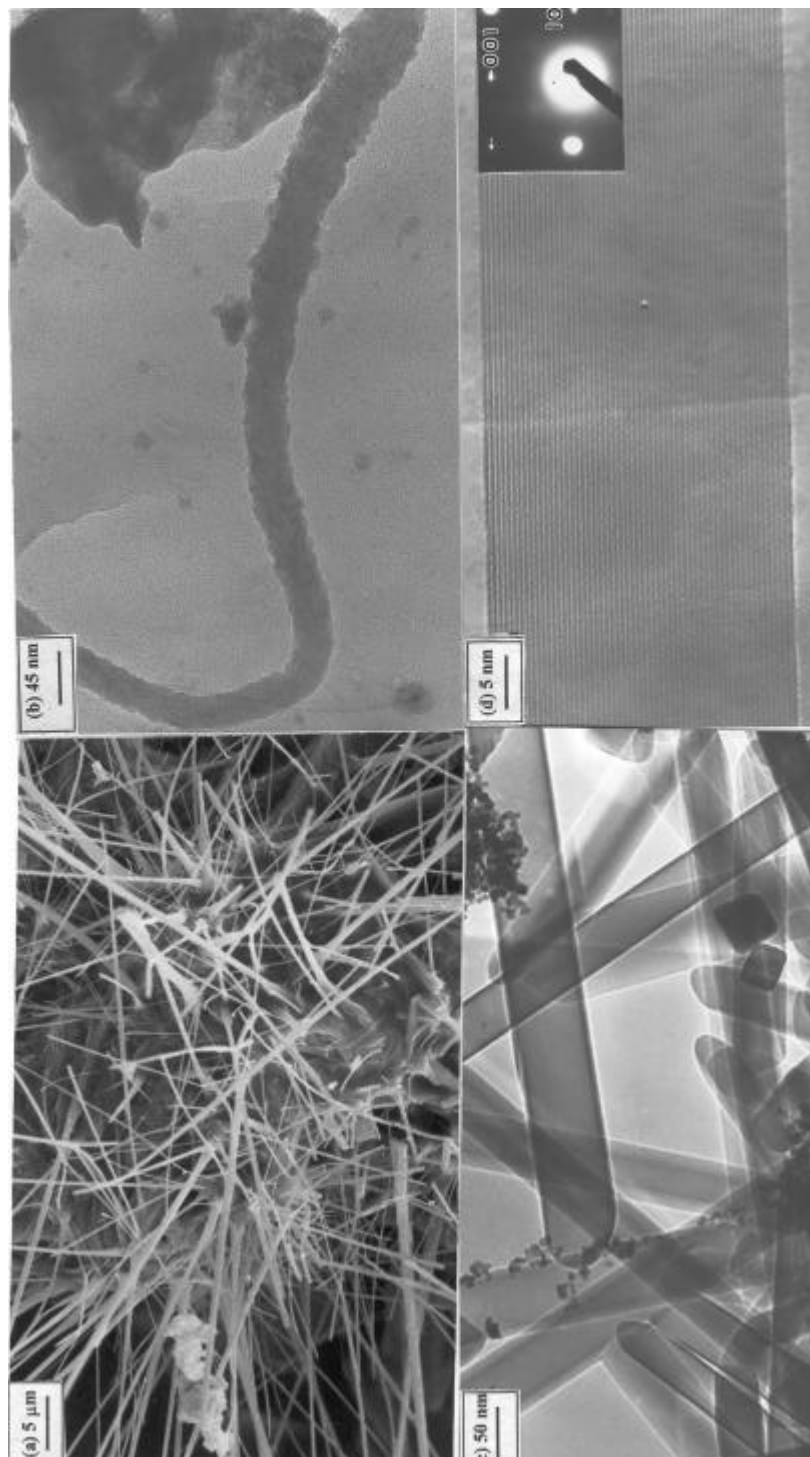


Figure 6. (a) SEM image of MoO_3 nanowires, (b) intermediate nanostructure of IrO_2 obtained on heat-treatment of the oxide-coated carbon nanotubes at 773 K, (c) nanowires of IrO_2 obtained after the complete removal of carbon template at 873 K for 12 h, and (d) HREM image of an IrO_2 single-crystalline nanowire showing the lattice planes. The SAED pattern of a nanowire is shown in the inset of (d).

tetragonal unit cell parameters, $a = 4.48 \text{ \AA}$ and $c = 3.12 \text{ \AA}$ (JCPDS file: 40-1290). IrO_2 also gave relatively good yield of nanowires. In figure 6b we also show an TEM image of the observed intermediate oxide structure, after heat treating the oxide-coated carbon nanotubes at 773 K. This temperature is slightly lower than that required for the complete removal of the carbon template. HREM observations in figure 6b also showed the polycrystalline nature of the intermediate nanostructure. It appears that during template removal, oxide coatings on neighboring carbon nanotubes coalesce to form wire-like nanostructures. Up to a certain temperature, the nanowire formed is polycrystalline, and becomes single crystalline around 873 K. This is seen from the TEM image of the IrO_2 nanowires in figure 6c. The diameters of the nanowires are in the range of 30–60 nm and length goes up to 1 μm . In figure 6d we show a HREM image that reveals the single crystalline nature of the IrO_2 nanowires. The image clearly shows (101) lattice planes. The inset in figure 6d shows the SAED pattern of a single nanowire, with the spots arising from the (100) and (001) planes of tetragonal IrO_2 . The XRD pattern reveals the rutile phase with the unit cell parameters, $a = 4.5 \text{ \AA}$ and $c = 3.15 \text{ \AA}$ (JCPDS file: 15-870). It is noteworthy that both RuO_2 and IrO_2 are metallic.

The formation of single crystalline nanowires in the present study is significant. A possible mechanism of formation of such nanowires may be as follows. CO or/and CO_2 is produced when oxide-coated carbon nanotubes are heated, the oxygen being (at least partly) derived from the coated oxide. Subsequently, the remaining metal or sub-oxide may get reoxidized and undergoes recrystallization. Another possibility is that the decomposition of the oxide precursor in the hot combustion zone of the nanotubes give rise to the crystals *in situ*. The crystals get elongated because of the evolution of gases during the transformation. The precursor decomposition also gives H_2O or/and CO_2 .

3.5 GaN nanowires

The GaN nanowires obtained by the various procedures described earlier all gave good XRD patterns characteristic of the wurtzite structure. The lattice constants obtained from the XRD patterns were $a = 3.18 \text{ \AA}$ and $c = 5.18 \text{ \AA}$, with minor differences. X-ray photoelectron spectra gave characteristic Ga(2p) and N(1s) signals. In figure 7a we show an SEM image of GaN nanowires obtained by procedure (i), wherein multi-walled carbon nanotubes were used as templates. The yield of the GaN nanowires by this procedure is excellent and the diameter of the majority of the nanowires is in the 35–50 nm range, but there were some in the 70–100 nm range. This variation occurs because of the nonuniformity in the nanotube diameter employed as templates. The length of the wires extends to a few microns. Most of the nanowires were straight although some odd shapes were encountered. The linear nanowires are generally single crystalline, showing a layer spacing of 0.276 nm corresponding to the [100] planes in the HREM image as demonstrated in figure 7b. The selected area electron diffraction (SAED) pattern of the linear nanowires (see inset of figure 7b), shows the Bragg spots due to the (100) reflection of the wurtzite structure. The (100) planes are nearly perpendicular to the growth direction. The normal to the (100) planes forms an acute angle of 10° with respect to the growth direction as shown in figure 7b.

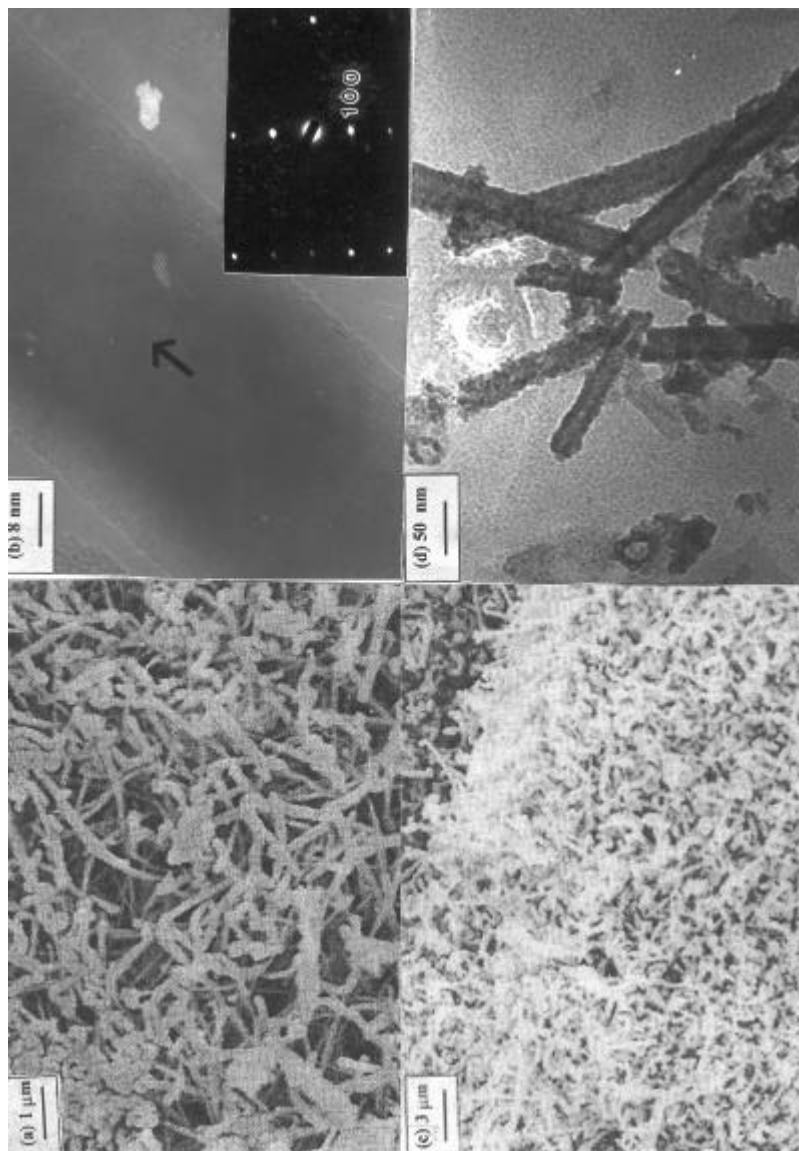


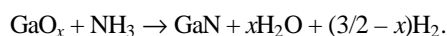
Figure 7. (a) SEM and (b) HREM images respectively of the GaN nanowires obtained by procedure (i), wherein MWNTs are used as templates. Inset in (b) shows the SAED pattern. The arrow in (b) is the growth direction, making an angle of $\sim 10^\circ$ with the normal to the (100) planes. (c) SEM image of the GaN nanowires obtained by procedure (ii) wherein catalytic nanoparticles are dispersed on silica. (d) Nanotube-like structures obtained with the use of the Ni catalyst in procedure (ii).

In figure 7c we show an SEM image of GaN nanowires obtained by procedure (ii) wherein the reaction of the gallium oxide and NH_3 was carried out in the presence of a catalytic Fe particles dispersed over silica. The yield of nanowires obtained by this procedure is also high. The diameters of the nanowires are in the 30–50 nm range and the lengths go up to several microns. This procedure yields good single-crystalline linear nanowires. HREM images reveal the characteristic 0.259 nm spacing between [002] planes. The SAED pattern shows Bragg spots corresponding to the [002] reflections of the wurtzite structure. The growth direction of the nanowires is perpendicular to the [002] planes. Use of the Ni catalyst instead of the Fe catalyst in procedure (ii) also gave satisfactory results. The diameters of nanowires got by this method are around 40 nm and lengths go up to several micrometres. We also obtained nanotube-like structures by this method as shown in figure 7d. GaN nanowires were also obtained by procedure (iii), wherein the reaction of NH_3 with the gallium oxide was carried out in the presence of Fe particles, but without the silica support. The yield of the nanowires by this procedure is not very high, indicating the importance of the role played by the silica support in procedure (ii). It appears that a homogeneous dispersion of the particles of Fe and gallium oxide over the silica support favours the formation of the nanowires. Furthermore, bulk particles of GaN mixed with the catalytic particles were found in the product, in the absence of the silica support. The length of the nanowires is of the order of few microns, but the diameter is rather large, varying between 70 and 200 nm. The morphology of the nanowires obtained by procedure (iii) is also not generally satisfactory. The growth direction of the nanowires in this procedure was exactly perpendicular to the [100] planes. Procedure (iii) with the Ni catalyst also yields thick nanowires (80–150 nm dia.).

GaN nanowires could also be prepared by the reaction of NH_3 with a homogeneous mixture of fine, high surface area $\text{Ga}_2\text{O}_3/\text{Fe}_2\text{O}_3$ particles, by employing the citrate method (iv). The diameter of the nanowires obtained by this method was around 70 nm. The nanowires were generally linear and single crystalline. We have also carried out the synthesis with Ni catalyst prepared by the citrate method. We could get good yields of long and uniform nanowires with lengths up to 15 microns and diameters in the 30–50 nm range by this method. HREM image of a GaN nanowire shows lattice planes with a spacing of 0.276 nm corresponding to the [100] planes of hexagonal GaN. SAED pattern of the nanowires shows the Bragg spot corresponding to the [100] reflection of the wurtzite structure. The direction of growth of the nanowires in this procedure was perpendicular to the [100] planes.

GaN nanowires prepared by the above procedures show satisfactory photoluminescence spectra. There is a characteristic emission band around 380 nm and weak feature around 530 nm. The observed PL features are comparable to those of bulk GaN which is known to exhibit a strong blue PL peak around 360 nm and a weaker yellow peak around 540 nm.

A few observations on the nature of the reactions occurring in the different procedures would be in order. The basic reaction involves the nitridation of the gallium oxide species produced *in-situ* by the decomposition of $\text{Ga}(\text{acac})_3$ in a reducing atmosphere. We represent the gallium oxide species as GaO_x , although it is likely to be Ga_2O . The reaction may be written as,



In procedure (i) the carbon nanotubes not only act as templates to confine the reaction and allow the growth of the GaN nanowire, but also take part in the reduction of the oxide. In procedures (ii)–(iv), catalytic Fe or Ni particles are present. Under the reaction conditions employed, it is likely that they had metallic Ni particles. The metal particles probably control the diameter of the nanowire by a directed flow of the reactant gases. Furthermore, since the transition metal probably dissolves both Ga and N, it can provide an appropriate nucleation centre for the growth of the GaN nanowires. We have found some evidence for the formation of clusters containing the metal from which the GaN nanowire emanates.

4. Other metal nanowires and nanotubes

Besides preparing CNTs and inorganic nanowires and nanotubes by using CNTs, we have synthesized and characterized other nanowires and nanotubes as well. Thus, we have been able to prepare nanowires of semiconductors such as ZnS, ZnSe, CdS, CdSe, CuS and CuSe by employing solvothermal reactions in the presence of surfactants⁸. Nanotubes of CdSe and CdS have also been obtained by this procedure⁹. Nanotubes and nanowires of materials such as MoS₂ and WS₂ have been obtained by the decomposition of trisulphides or ammonium salts in a hydrogen atmosphere¹⁰. These materials were prepared earlier by Tenne *et al*¹¹ starting with the oxides, wherein the trioxides were first heated at high temperatures in N₂ + H₂ and then in H₂S + H₂. The trisulphide route has been employed to prepare NbS₂ nanotubes for the first time¹².

Acknowledgements

The authors thank Drs B C Satishkumar and R Sen, Ms M Nath and Mr F L Deepak for their collaboration, and the Defence Research & Development Organization for support.

References

1. Iijima S 1991 *Nature (London)* **354** 56
2. Rao C N R, Satishkumar B C, Govindaraj A and Nath M 2001 *Chem. Physchem.* **2** 78
3. Sen R, Govindaraj A and Rao C N R 1997 *Chem. Phys. Lett.* **267** 276; Rao C N R, Sen R, Satishkumar B C and Govindaraj A 1998 *Chem. Commun.* 1525
4. Satishkumar B C, Thomas P J, Govindaraj A and Rao C N R 2000 *Appl. Phys. Lett.* **77** 2530
5. Govindaraj A, Satishkumar B C, Nath M and Rao C N R 2000 *Chem. Mater.* **12** 202
6. Satishkumar B C, Govindaraj A, Nath M and Rao C N R 2000 *J. Mater. Chem.* **10** 2115
7. Deepak F L, Govindaraj A and Rao C N R 2001 *J. Nanosci. Nanotech.* **1** 303
8. Govindaraj A, Deepak F L, Gunari N A and Rao C N R 2001 *Israel J. Chem.* (nanotechnology special issue) **41** (in press)
9. Rao C N R, Govindaraj A, Deepak F L, Gunari N A and Nath M 2001 *Appl. Phys. Lett.* **78** 1853
10. Nath M, Govindaraj A and Rao C N R 2001 *Adv. Mater.* **13** 283
11. Feldman Y, Wasserman E, Srolovitch D J and Tenne R 1995 *Science* **267** 222
12. Nath M and Rao C N R 2001 *J. Am. Chem. Soc.* **123** 4841